Stem Cell Reports
Report
OPEN ACCESS

Inhibition of IKK/NF-κB Signaling Enhances Differentiation of Mesenchymal Stromal Cells from Human Embryonic Stem Cells

Peng Deng,[1] Chenchen Zhou,[1] Ruth Alvarez,[1] Christine Hong,[2,*] and Cun-Yu Wang[1,3,*]
[1]Laboratory of Molecular Signaling, Division of Oral Biology and Medicine, School of Dentistry, University of California, Los Angeles, Los Angeles, CA 90095, USA
[2]Section of Orthodontics, Division of Growth and Development, School of Dentistry, University of California, Los Angeles, Los Angeles, CA 90095, USA
[3]Department of Bioengineering, Henry Samueli School of Engineering and Applied Science, University of California, Los Angeles, Los Angeles, CA 90095, USA
*Correspondence: chong@dentistry.ucla.edu (C.H.), cwang@dentistry.ucla.edu (C.-Y.W.)
http://dx.doi.org/10.1016/j.stemcr.2016.02.006

SUMMARY

Embryonic stem cell-derived mesenchymal stromal cells (MSCs; also known as mesenchymal stem cells) represent a promising source for bone regenerative medicine. Despite remarkable advances in stem cell biology, the molecular mechanism regulating differentiation of human embryonic stem cells (hESCs) into MSCs remains poorly understood. Here, we report that inhibition of IκB kinase (IKK)/nuclear factor kappa B (NF-κB) signaling enhances differentiation of hESCs into MSCs by expediting the loss of pluripotent markers and increasing the expression of MSC surface markers. In addition, a significantly higher quantity of MSCs was produced from hESCs with IKK/NF-κB suppression. These isolated MSCs displayed evident multipotency with capacity to terminally differentiate into osteoblasts, chondrocytes, and adipocytes in vitro and to form bone in vivo. Collectively, our data provide important insights into the role of NF-κB in mesenchymal lineage specification during hESC differentiation, suggesting that IKK inhibitors could be utilized as an adjuvant in generating MSCs for cell-mediated therapies.

INTRODUCTION

Human mesenchymal stromal cells (MSCs; also known as mesenchymal stem cells) have gained considerable attention for their promising potential in cell-mediated therapy. MSCs are progenitor cells whose capacity to differentiate into osteoblasts and modulate the immune response makes them instrumental in bone regenerative medicine (Kode et al., 2009; Stappenbeck and Miyoshi, 2009; Alvarez et al., 2015; Deng et al., 2015). Clinical trials have already demonstrated that implantation of MSCs is an effective and safe treatment modality in defect repair (Bianco et al., 2013; Quarto et al., 2001; Wang et al., 2012). Although MSCs used in cell therapies are mostly isolated from adult bone marrow, proliferation and differentiation capacity of these MSCs from bone marrow (BMSCs) has been shown to decline as the donor patient ages (Kern et al., 2006; Quarto et al., 2001). Due to these shortcomings of BMSCs, human embryonic stem cells (hESCs), which have the potential to provide an unlimited supply of MSCs, are potential alternative sources for MSCs (Choo and Lim, 2011; Thomson, 1998). hESC-derived MSCs are similar to BMSCs biologically and functionally, but with higher osteogenic potential and proliferation rates as well as less immunogenicity (Li et al., 2013). Three methods have been developed to promote the differentiation of hESCs into MSCs: (1) the formation of three-dimensional embryonic bodies, (2) the culture of hESCs on stromal cells, and (3) the culture of hESCs as monolayers (Arpornmaeklong et al., 2009; Barberi et al., 2005; Villa-Diaz et al., 2012; Karp et al., 2006). However, the molecular mechanism by which hESCs commit to MSC fate remains elusive.

The nuclear factor kappa B (NF-κB) is known for its key role in the regulation of many cellular processes. The classical NF-κB is a heterodimer of p50 and p65/RelA proteins, in which the p65/RelA subunit has transactivation activity. The IκB kinase (IKK) complex mediates the degradation of IκBs to activate NF-κB (Krum et al., 2010). Recent studies have suggested that NF-κB may also play a role in stem cell self-renewal and differentiation (Armstrong et al., 2006; Dreesen and Brivanlou, 2007). The NF-κB subunits, including p65, p50, IκBα, and IκBβ, were found to be present throughout differentiation of hESCs (Yang et al., 2010). Although NF-κB signaling activity is low in hESCs, its inhibition leads to significant cell differentiation (Armstrong et al., 2006), suggesting that basal level of NF-κB activity is required for hESC identity. On the other hand, p65 overexpression caused loss of pluripotency and hESC differentiation (Luningschror et al., 2012). Moreover, it has been shown that Nanog maintains the pluripotency of mouse ESCs by binding to and suppressing the functions of NF-κB transcriptional activity (Torres and Watt, 2008). Given these seemingly contradictory reports, the precise regulatory functions of NF-κB in hESC differentiation require further investigation.

In this report, we investigated the effect of IKK/NF-κB signaling in regulating differentiation of hESCs into MSCs. Here, we demonstrated that inactivation of the

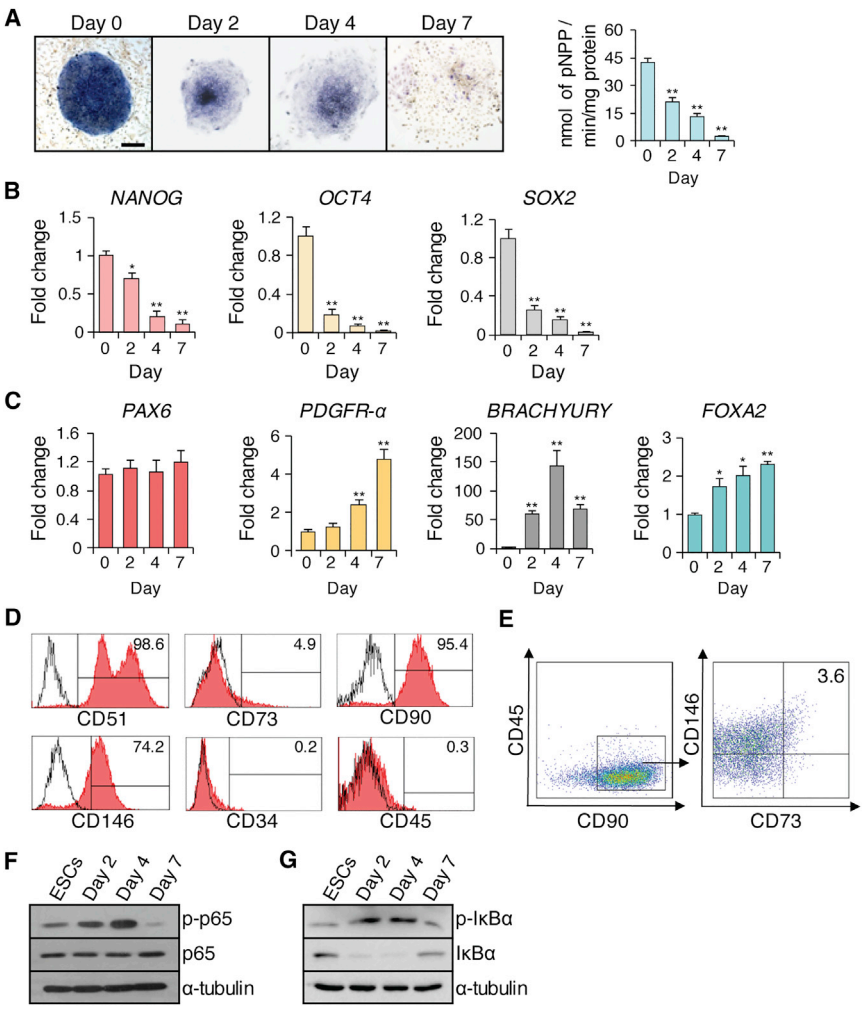

Figure 1. Spontaneous Differentiation of hESCs without the Feeder Cell Layer

(A) Alkaline phosphatase staining and quantitative alkaline phosphatase activity assay at 0, 2, 4, and 7 days. Scale bar indicates 200 μm.

(B) qRT-PCR results of pluripotent markers (*NANOG*, *OCT4*, *POU5F1*) at 0, 2, 4, and 7 days.

(C) qRT-PCR results of an ectodermal gene (*PAX6*), mesodermal genes (*PDGFR-α* and *BRACHYURY*), and an endodermal gene (*FOXA2*) at 0, 2, 4, and 7 days.

(D) Flow cytometry analysis of cells expressing MSC surface markers.

(E) Four-color flow cytometry analysis for CD45, CD90, CD73, and CD146 expression was used to isolate $CD73^+CD90^+CD146^+CD45^-$ MSCs.

(F) Western blot of p65 and phosphorylated p65 at 0, 2, 4, and 7 days of hESC differentiation.

(G) Western blot of IκBα and phosphorylated IκBα at 0, 2, 4, and 7 days of H1 hESC differentiation. Three independent experiments were performed.

*$p < 0.05$, **$p < 0.001$.

IKK/NF-κB signaling pathway by the small-molecule IKK inhibitor (IKKi) and p65 knockdown promotes hESC differentiation into MSCs on monolayer culture. IKKi-treated hESCs generated a significantly increased MSC population and exhibited multipotency.

RESULTS

Inhibition of NF-κB Signaling Promotes hESC Differentiation and Enhances MSC Marker Expression

hESCs can be differentiated into MSCs when they are cultured in a monolayer without feeder cells (Karp et al., 2006). To induce this differentiation, we seeded the H1 hESC aggregates onto tissue culture dishes without feeder cells. We found that the alkaline phosphatase activity of hESCs decreased progressively and dramatically in the 7 days following culturing in a monolayer (Figure 1A). Real-time RT-PCR revealed that the expression of pluripotent markers, including *NANOG*, *OCT4*, and *SOX2*, gradually declined in parallel with alkaline phosphatase activity, indicating hESC differentiation (Figure 1B).

We then examined the expression pattern of markers indicative of the three germ layers. While the ectodermal marker gene *PAX6* was not induced, the endodermal marker gene *FOXA2* and two mesodermal markers *PDGFR-α* and *BRACHYURY* were significantly elevated upon monolayer culture, indicating their preferential differentiation toward these two specific lineages (Figure 1C). Furthermore, when the MSC surface markers were assessed after 7 days of differentiation, more than 95% of cells were positive for CD51 and CD90, but negative for CD34 and CD45 (Figure 1D). However, $CD146^+$ cells were 74.2% and $CD73^+$ cells were relatively low at 4.9% (Figure 1D). Based on these results, we selected the combination markers of $CD73^+CD90^+CD146^+CD45^-$ to isolate MSCs, excluding CD51 due to its high level of expression at 99% (Figure 1D). We were able to obtain 3.6%

$CD73^+CD90^+CD146^+CD45^-$ MSCs of the total differentiated cells from H1 hESCs (Figure 1E). Similarly, MSCs could also be generated from H9 hESCs (Figures S1A–S1E).

IKK directly phosphorylates the p65 transactivation domain on serine 536 (S536), a process that is correlated with IKK/NF-κB activity (Yang et al., 2003). To examine the status of the IKK/NF-κB signaling pathway, we screened for phosphorylated p65 during hESC differentiation. Consistent with previous studies (Foldes et al., 2010; Kang et al., 2007), phosphorylated status of p65 and IκBα was low, suggesting that NF-κB activity is present but low in H1 hESCs (Figures 1F and 1G). Interestingly, phosphorylation of p65 and IκBα increased progressively in the first 4 days of H1 or H9 hESC differentiation, but decreased to the basal level on day 7 (Figures 1F, 1G, and S1F). In contrast, the components of non-canonical NF-κB signaling, p100 and p52 (Bakkar et al., 2012), were minimally affected (Figure S1G).

To determine whether IKK/NF-κB signaling plays a functional role in hESC differentiation into MSCs, we used IKKi to inhibit the IKKβ subunit of IKK complex, blocking IKK-mediated phosphorylation-induced proteasomal degradation of IκB, and thereby disabling activation of NF-κB (Baxter et al., 2004; Park et al., 2006). We treated the H1 hESC monolayer culture daily with IKKi (1 μM) from day 1 to day 4 during which IKK/NF-κB activity was found to be upregulated. This treatment resulted in significant inhibition of p65 and IκBα phosphorylation (Figures 2A and 2B), as well as reduction in alkaline phosphatase activity (Figure 2C) compared with vehicle control at days 2 and 4 of H1 hESC differentiation. Similarly, during the 7-day differentiation period, IKKi treatment consistently expedited the loss of pluripotency in H1 hESCs as determined by further suppressed mRNA expression levels of pluripotent markers, including *NANOG*, *OCT4*, and *SOX2* (Figure 2D). Germ layer marker examination revealed that mesodermal markers *PDGFR-α* and *BRACHYURY* were found to be significantly upregulated as a result of treatment at days 2 and 4 of hESC differentiation (Figure 2E). The endodermal marker *FOXA2* was also upregulated at day 4 (Figure 2E). In contrast, the ectodermal marker *PAX6* gene expression remained unchanged (Figure 2E). MSC marker assessment showed that *CD73* and *CD146* were significantly upregulated following 4 days of IKKi treatment (Figure 2F); such upregulation was further confirmed by flow cytometry analysis (Figure 2G). IKKi treatment also generated a 3-fold increase in the proportion of $CD73^+CD90^+CD146^+CD45^-$ MSCs in the total differentiated H1 hESC population, compared with vehicle control treatment (Figure 2H). Similarly, we found that IKKi treatment also significantly generated more MSCs from H9 hESCs (Figure S2).

IKKi-Treated Cells Exhibit Enhanced Osteogenic and Chondrogenic Potentials

As IKKi treatment during hESC differentiation generated a larger $CD73^+CD90^+CD146^+CD45^-$ MSC population, we examined whether inhibiting NF-κB signaling by IKKi enhances terminal differentiation capacity of differentiated hESCs. After H1 hESCs were grown in monolayer culture for 7 days with and without IKKi, these differentiated and unsorted hESCs were further induced to undergo osteogenic differentiation with osteogenic induction (OI) medium in the absence of IKKi for 7 days. As shown in Figure S3A, alkaline phosphatase activity was significantly elevated in IKKi-pretreated cells compared with control cells. In addition, real-time RT-PCR showed elevated expression levels of osteogenic markers, including *RUNX2* and *BGLAP* (Figure S3B). Consistent with 7-day osteogenic induction results, IKKi-pretreated cells were able to form more mineralized nodules than control cells after prolonged treatment with OI medium for 14 days as demonstrated by Alizarin red staining (Figure S3C).

Furthermore, we evaluated and compared the chondrogenic capacity of differentiated H1 hESCs under chondrogenic conditions. IKKi-pretreated cells showed the presence of increased glycosaminoglycans as demonstrated by Alcian blue staining following prolonged treatment with chondrogenic induction medium for 21 days (Figure S3D). mRNA expression levels of chondrogenic marker genes including *SOX9* and *COL2A1* were also significantly upregulated (Figure S3E).

Inhibition of NF-κB Signaling by p65 Depletion Promotes hESC Differentiation and Enhances MSC Marker Expression

To further confirm that inhibition of NF-κB promotes hESC differentiation, we knocked down p65 in hESCs using lentiviruses expressing p65 small hairpin RNAs (shRNAs), targeting the 3′ UTR. The depletion of p65 in H1 hESCs was confirmed by real-time RT-PCR (Figure 3A) and by significantly suppressed expression of NF-κB target genes, including *cIAP2*, *IL-6*, and *IL-8* (Figure 3B). Consistent with our IKKi treatment results, this p65 deficiency showed the decline of alkaline phosphatase activity at days 2 and 4 of the differentiation process (Figure 3C). Moreover, real-time RT-PCR revealed accelerated loss of the pluripotent markers *NANOG*, *OCT4*, and *SOX2* during hESC differentiation (Figure 3D). As with IKKi treatment, the endodermal marker *FOXA2* and two mesodermal markers *PDGFR-α* and *BRACHYURY* were found to be significantly elevated while the ectodermal marker *PAX6* was unchanged (Figure 3E). The expression of *CD73* and *CD146* was also significantly upregulated in a time-dependent manner, with the most drastic differences at day 7 of hESC differentiation (Figure 3F). Flow cytometry analysis confirmed the increased

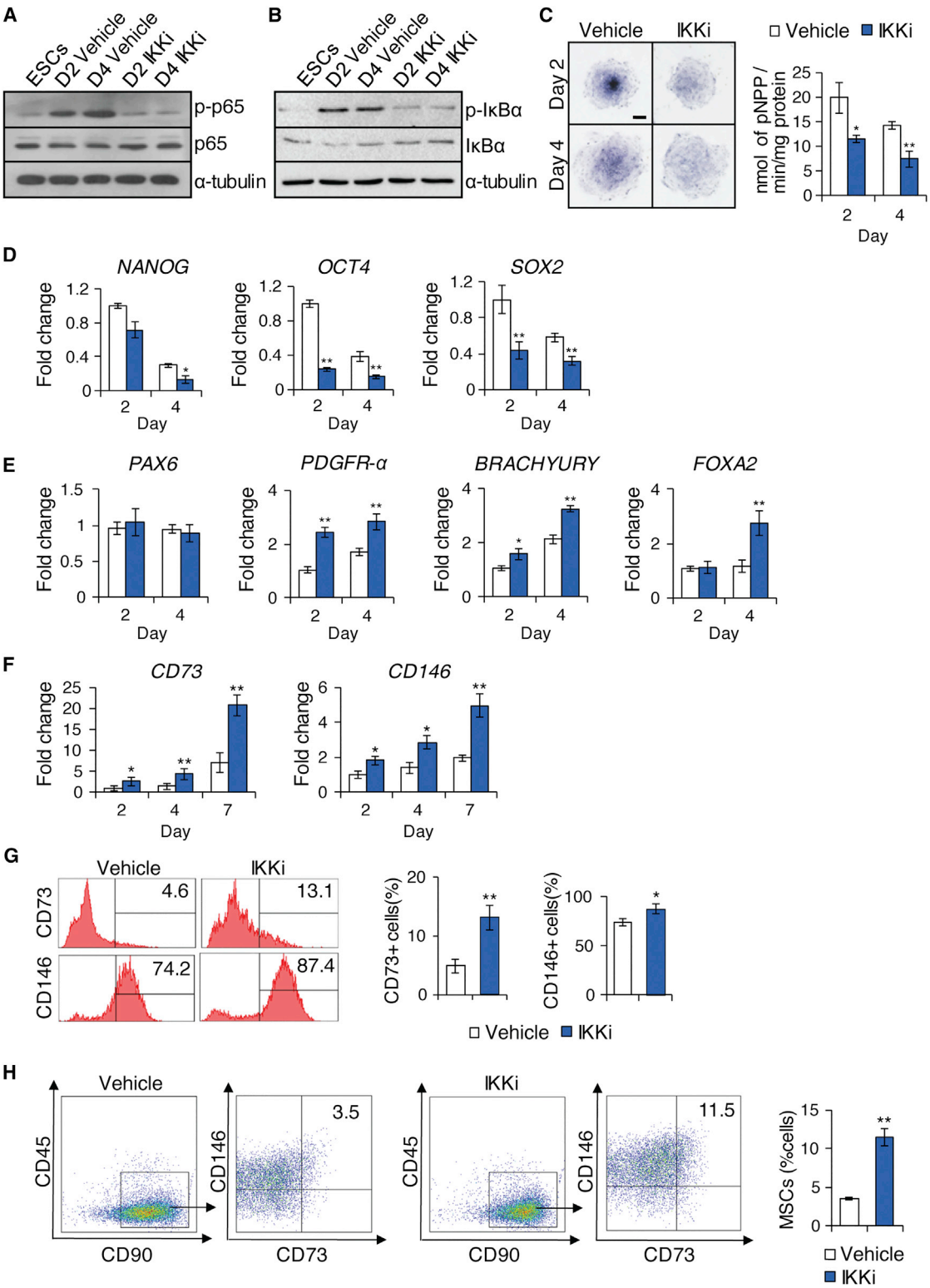

Figure 2. Effect of IKKi Treatment on Mesenchymal Lineage Specification of hESCs

(A) Western blot of p65 and phosphorylated p65 at 0, 2, and 4 days of hESC differentiation.

(B) Western blot of IκBα and phosphorylated IκBα at 0, 2, and 4 days of hESC differentiation.

(C) Alkaline phosphatase staining and quantitative alkaline phosphatase activity assay at 2 and 4 days. Scale bar indicates 200 μm.

(legend continued on next page)

expression of CD73 and CD146 (Figure 3G). Finally, similar to IKKi treatment, NF-κB inhibition by p65 depletion increased the proportion of $CD73^+CD90^+CD146^+CD45^-$ MSCs by 3-fold (Figure 3H).

MSCs Derived from IKKi-Treated hESCs Maintain Multipotency In Vitro and Form Bone In Vivo

Since IKKi treatment generated significantly more MSCs from hESCs, it was important to determine whether these MSCs maintained multipotential properties and formed bone tissues in vivo. We sorted MSCs derived from IKKi-treated H1 hESCs and vehicle-treated hESCs and compared the terminal differentiation capacity to develop into osteoblasts, chondrocytes, and adipocytes in the absence of IKKi. Induced to undergo osteogenic differentiation, both groups displayed similar alkaline phosphatase activity and mineralization capacity (Figures 4A and 4C). Real-time RT-PCR also showed no significant differences in the expression of the osteogenic marker genes, *RUNX2* and *BGLAP* (Figure 4B). Similarly, no significant changes were observed in chondrogenic potential, as determined by Alcian blue staining and expression of the chondrogenic marker genes, *SOX9* and *COL2A1* (Figures 4D and 4E). Induced to undergo adipogenic differentiation with adipogenic induction media for 21 days, oil red O staining revealed lipid deposit formation (Figure 4F) and the quantification and expression of adipogenic marker genes, *PPAR-γ* and *LPL*, showed no difference in adipogenic potential between the two groups (Figures 4F and 4G). Importantly, both populations were able to form bone in vivo (Figure 4H). To confirm ectopic bone regeneration, we examined the expression of human osteocalcin in these mineralized tissues. Osteocytes and lining osteoblasts were positively stained in both groups (Figure S4). To examine whether IKKi treatment might induce chromosomal abnormality at the genomic level, we performed G-banded chromosome studies of 20 mitoses. The results revealed that both groups exhibited a normal male karyotype with no gross abnormalities (Figure 4I).

DISCUSSION

For successful utilization of hESCs to generate MSCs for cell-mediated therapies, it is critical to develop a better understanding of the molecular mechanisms that govern their differentiation into specific progenitor cells. Here, we identified an important mechanism that facilitates differentiation of pluripotent hESCs into multipotent MSCs. By inhibiting the NF-κB signaling pathway, hESCs were differentiated more readily into MSCs, thereby enhancing lineage-specific terminal differentiation into osteoblasts and chondrocytes.

Recent studies have suggested that NF-κB signaling is involved in both maintenance and differentiation of ESCs (Dreesen and Brivanlou, 2007). While a low but detectable level of NF-κB activity was found in both mouse ESCs (mESCs) and hESCs (Torres and Watt, 2008; Yang et al., 2010), the functional role of NF-κB signaling was found to be contradictory. In mESCs, endogenous NF-κB activity and target gene expression was observed to have increased during the differentiation process. In addition, forced expression of the NF-κB subunit p65 caused mESC differentiation and loss of pluripotency (Luningschror et al., 2012). Conversely, NF-κB inhibition in mice increases expression of pluripotency markers (Dutta et al., 2011). miR-290, an ESC-specific microRNA cluster that targets p65, maintains pluripotency in mESCs by repressing NF-κB signaling (Luningschror et al., 2012). Similarly, Nanog's binding to NF-κB inhibits the transcriptional activity of NF-κB and collaborates with Stat3 to promote self-renewal and impair differentiation (Torres and Watt, 2008). In contrast, it is reported that NF-κB inhibition in hESCs leads to hESC differentiation and loss of pluripotency (Armstrong et al., 2006). Using two different approaches for inhibiting NF-κB, our findings confirmed the notion that NF-κB inhibition promoted hESC differentiation. Importantly, we found that inhibition obtained significantly higher yields of MSCs. It was reported that there was a significant increase in expression of the NF-κB pathway components, p50 and phosphorylated form of p65, during embryonic body-mediated differentiation of hESCs grown in mouse embryonic feeder (MEF) layers (Yang et al., 2010). Similarly, here we demonstrated an increase in phosphorylated p65, indicative of heightened IKK/NF-κB activity, as hESCs differentiated in the monolayer culturing system and lost their pluripotency. It is noteworthy that such heightened activity was present only during the initial 4 days of differentiation and quickly

(D) qRT-PCR results of *NANOG*, *OCT4*, and *POU5F1* at 2 and 4 days.
(E) qRT-PCR results of *PAX6*, *PDGFR-α*, *BRACHYURY*, and *FOXA2* at 2 and 4 days.
(F) qRT-PCR results of *CD73* and *CD146* at 2, 4, and 7 days.
(G) Flow cytometry analysis of cells with or without IKKi treatment examining MSC marker expression.
(H) Four-color flow cytometry analysis for CD45, CD90, CD73, and CD146 expression to isolate $CD73^+CD90^+CD146^+CD45^-$ MSCs following 7 days of hESC differentiation with or without IKKi. Proportions of $CD73^+CD90^+CD146^+CD45^-$ MSCs generated. Three independent experiments were performed.
*$p < 0.05$, **$p < 0.001$.

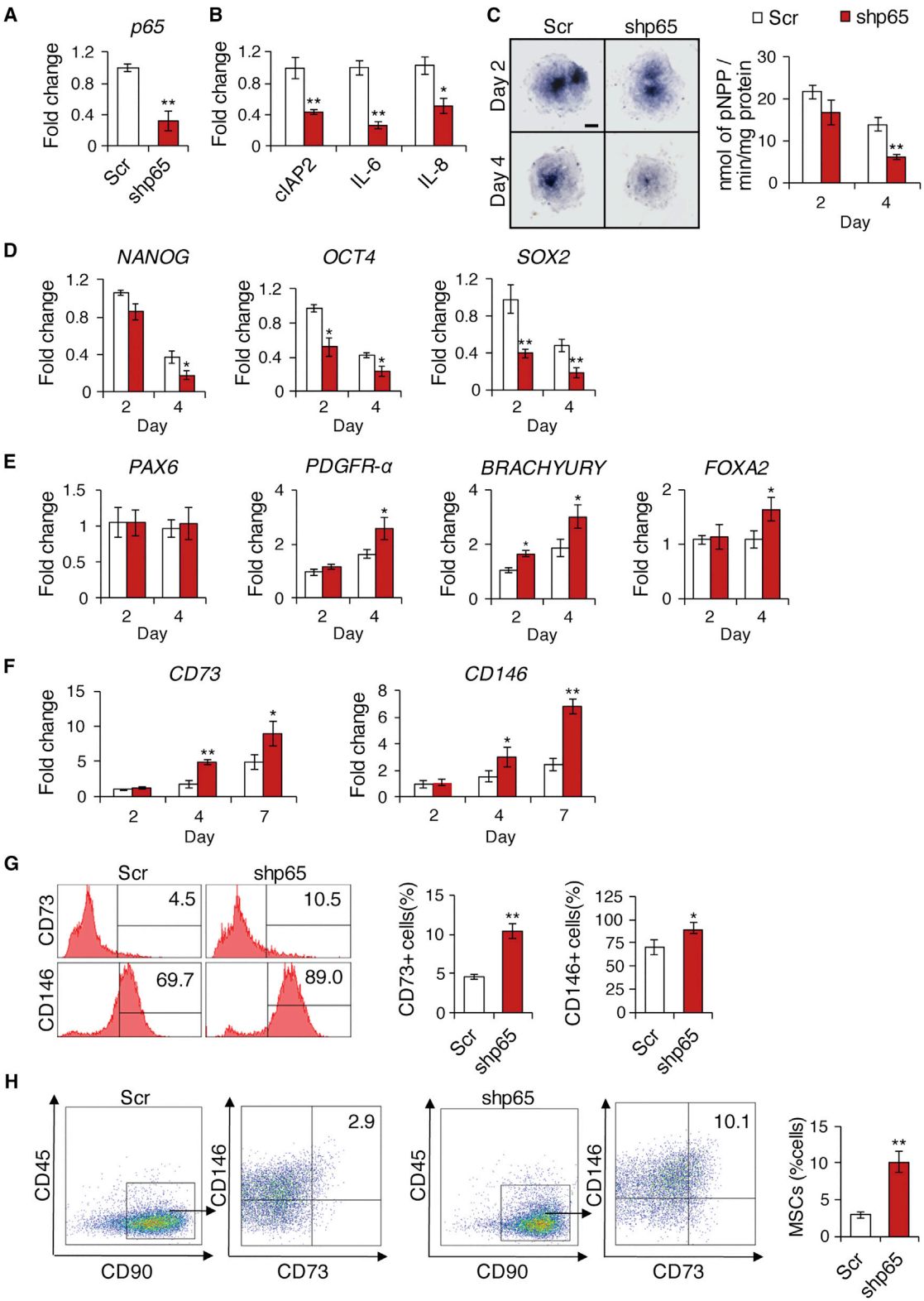

Figure 3. Effect of p65 Knockdown on Differentiation and Mesenchymal Lineage Specification of hESCs

(A) qRT-PCR showing the deletion of *p65* mRNA by shp65 in H1 hESCs.

(B) qRT-PCR results of NF-κB target genes (*cIAP2*, *IL-6*, *IL-8*) in Scr or shp65 transduced H1 hESCs at 4 days.

(legend continued on next page)

returned to the basal level. When this transient upregulation of IKK/NF-κB signaling was inhibited, hESC differentiation was enhanced, suggesting that IKK/NF-κB activity may act as a compensatory mechanism to suppress its differentiation into progenitor cells during the early stages. Indeed, such a compensatory mechanism was also seen in previous studies. NF-κB activity is high during the development of bone but decreases in adult bone (Krum et al., 2010). Previously, we have found that the inhibition of NF-κB signaling promotes osteogenic differentiation of MSCs in vivo and in vitro (Chang et al., 2009, 2013). Altogether, our results suggest that NF-κB is a negative regulator of MSC differentiation from ESCs and bone formation.

It has previously been reported that differentiation of hESCs without the embryonic body stage led to an increase in the capacity of hESCs to differentiate into osteogenic progenitor cells (Karp et al., 2006). Consistent with these findings, our differentiation culture method resulted in cells with increased mesodermal and endodermal lineage marker gene expression, while the expression of the ectodermal lineage marker, *PAX6*, was unchanged. These results differ distinctly from embryonic bodies in which the inhibition of NF-κB promotes ectodermal lineage alone. Such discrepancies may stem from differences in culturing conditions including dosing. Yang et al. (2010) used a 20 μM dose of IKKi daily for 6 days, which is significantly higher than the concentration used in this study, 1 μM. This super-physiological concentration of IKKi may be responsible for the significant cell death and morphology changes that Yang et al. (2010) observed in hESCs. During our dosing optimization studies, we initially experienced massive cell death with higher doses, leading us to decide on a 1 μM dose. While IKKi at this low dose not only induces minimal cell death and proliferation impairment, it is sufficient to significantly suppress IKK activity, as demonstrated by a reduction in the S536 phosphorylated form of p65. As such, evaluating the role of NF-κB signaling by directly comparing different culturing conditions warrants closer examination.

In summary, we demonstrated that hESCs are a reliable resource to generate functional MSCs, making hESC-derived MSCs a promising alternative to BMSCs, which require invasive harvesting and show diminishing differentiation capacity with age. We also provide evidence that inhibition of NF-κB signaling promotes differentiation of hESCs into MSCs. By inhibiting IKK/NF-κB signaling, greater quantities of MSCs can be obtained more efficiently. Purified MSCs generated with IKKi treatment had the capacity for in vivo bone formation, offering tremendous benefits for bone tissue engineering. Therefore, the use of IKKi to inhibit NF-κB signaling to derive and enrich functional MSCs from hESCs may represent an efficient method that holds great promise for regenerative medicine in the future.

EXPERIMENTAL PROCEDURES

Cell Culture

hESC-related work was approved by UCLA Embryonic Stem Cells Research Oversight Committee (IRB: 10-001711-CR-00001). H1 and H9 hESCs were obtained from UCLA Broad Stem Cell Research Center. hESCs (passages 35–45) were cultured on a mitotically inactivated MEF layer, as previously described (Thomson, 1998). To induce differentiation of hESCs, we detached hESC colonies using type IV collagenase (1 mg/ml), and hESC aggregates were plated into tissue culture dishes and grown in DMEM, containing 15% fetal bovine serum, 1% L-glutamine, 1% non-essential amino acid, and 1% penicillin-streptomycin for 1 day. Subsequently, IKKi (1 μM, Calbiochem) was added during ESC differentiation as indicated. After 7 days of differentiation, the derived cells were trypsinized to generate a single-cell suspension for further differentiation.

shRNA Knockdown

To knockdown p65 during differentiation of hESCs, we packaged and generated the lentiviruses expressing shRNA p65 or scramble shRNA (Scr) in 293T cells as described previously (Ramadoss et al., 2011). For viral infection, ESC aggregates were plated overnight and then infected with lentiviruses in the presence of polybrene (6 μg/ml) for 24 hr. After 3 days of infection, pools of colonies were selected with puromycin (Thermo Fisher Scientific) for 3 days at a concentration of 0.4 μg/ml. The target sequence for p65 shRNA was 5′-GTGACAAGGTGCAGAAAGA-3′.

All procedures were performed in accordance with the approved protocol by the University of California, Los Angeles (UCLA), and were oversight by UCLA Animal Research Committee (ARC). Detailed procedures are listed in Supplemental Experimental Procedures.

(C) Alkaline phosphatase staining and quantitative alkaline phosphatase activity assay for hESCs after transfection with Scr or shp65 lentivirus at 2 and 4 days. Scale bar indicates 200 μm.
(D) qRT-PCR results of *NANOG*, *OCT4*, and *POU5F1* at 2 and 4 days.
(E) qRT-PCR results of *PAX6*, *PDGFR-α*, *BRACHYURY*, and *FOXA2* at 2 and 4 days.
(F) qRT-PCR results of *CD73* and *CD146* at 2, 4, and 7 days.
(G) Flow cytometry analysis of cells expressing MSC markers.
(H) Four-color flow cytometry analysis for CD45, CD90, CD73, and CD146 to isolate $CD73^{+}CD90^{+}CD146^{+}CD45^{-}$ MSCs following 7 days of H1 hESC differentiation. Three independent experiments were performed.
*$p < 0.05$, **$p < 0.001$.

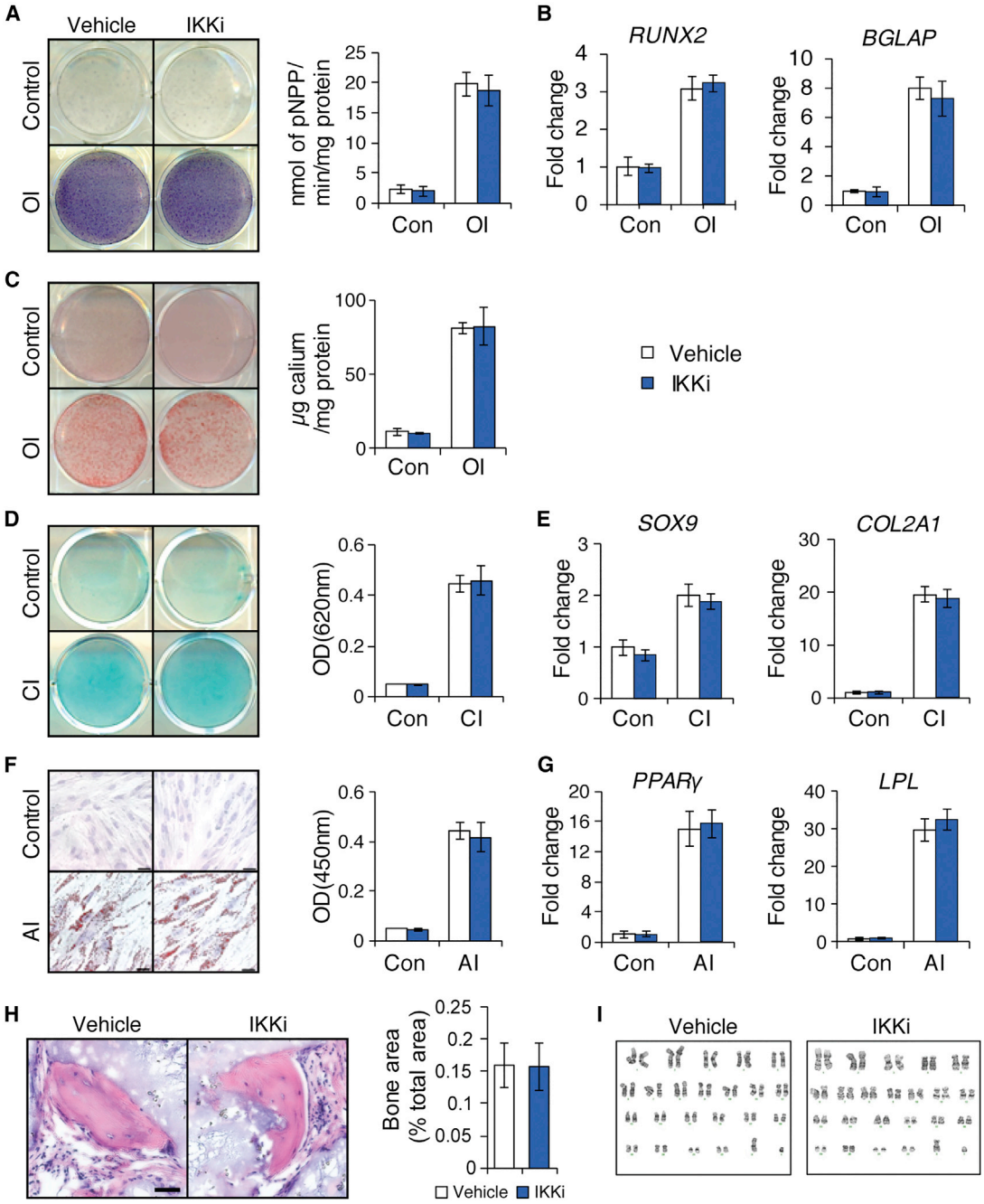

Figure 4. Characterization of Sorted MSCs Derived from IKKi-Treated hESCs

(A) Alkaline phosphatase staining and quantitative alkaline phosphatase activity assay after 14 days of osteogenic induction (OI).

(B) qRT-PCR results of osteogenic markers (*RUNX2* and *BGLAP*) after 7 days of OI.

(C) ARS staining and quantification after 14 days of OI.

(D) Alcian blue staining and quantification after 21 days of chondrogenic induction.

(E) qRT-PCR results of chondrogenic markers (*SOX9* and *COL2a1*) expression after 14 days of chondrogenic induction (CI).

(F) Oil red O staining and quantification after 21 days of adipogenic induction (AI). Scale bar indicates 200 μm.

(G) qRT-PCR results of adipogenic markers (*PPAR-γ* and *LPL*) expression after 14 days of AI.

(H) Bone formation in vivo by sorted MSCs derived from IKKi-treated H1 hESCs in six immunocompromised mice. Bar indicates 100 μm.

(I) Karyotype analysis of sorted MSCs derived from IKKi-treated H1 hESCs. For all in vitro experiments, three independent experiments were performed.

SUPPLEMENTAL INFORMATION

Supplemental Information includes Supplemental Experimental Procedures, four figures, and one table and can be found with this article online at http://dx.doi.org/10.1016/j.stemcr.2016.02.006.

AUTHOR CONTRIBUTIONS

D.P., C.Z., and R.A. performed the experiments and analyzed the data. C.H. and C.Y.W. designed experiments and wrote the manuscript.

ACKNOWLEDGMENTS

This work was supported by the UCLA Eli & Edythe Broad Center of Regenerative Medicine and Stem Cell Research Innovation Award and NIH/NIDCR grant R01DE016513. We thank Dr. Jinghua Tang for technical support on cell culture.

Received: October 29, 2015
Revised: February 5, 2016
Accepted: February 8, 2016
Published: March 10, 2016

REFERENCES

Alvarez, R., Lee, H.L., Wang, C.Y., and Hong, C. (2015). Characterization of the osteogenic potential of mesenchymal stem cells from human periodontal ligament based on cell surface markers. Int. J. Oral Sci. *7*, 213–219.

Armstrong, L., Hughes, O., Yung, S., Hyslop, L., Stewart, R., Wappler, I., Peters, H., Walter, T., Stojkovic, P., Evans, J., et al. (2006). The role of PI3K/AKT, MAPK/ERK and NFkappabeta signalling in the maintenance of human embryonic stem cell pluripotency and viability highlighted by transcriptional profiling and functional analysis. Hum. Mol. Genet. *15*, 1894–1913.

Arpornmaeklong, P., Brown, S.E., Wang, Z., and Krebsbach, P.H. (2009). Phenotypic characterization, osteoblastic differentiation, and bone regeneration capacity of human embryonic stem cell-derived mesenchymal stem cells. Stem Cells Dev. *18*, 955–968.

Bakkar, N., Ladner, K., Canan, B.D., Liyanarachchi, S., Bal, N.C., Pant, M., Periasamy, M., Li, Q., Janssen, P.M., and Guttridge, D.C. (2012). IKKα and alternative NF-κB regulate PGC-1β to promote oxidative muscle metabolism. J. Cell Biol. *196*, 497–511.

Barberi, T., Willis, L.M., Socci, N.D., and Studer, L. (2005). Derivation of multipotent mesenchymal precursors from human embryonic stem cells. PLoS Med. *2*, e161.

Baxter, A., Brough, S., Cooper, A., Floettmann, E., Foster, S., Harding, C., Kettle, J., McInally, T., Martin, C., Mobbs, M., et al. (2004). Hit-to-lead studies: the discovery of potent, orally active, thiophene carboxamide IKK-2 inhibitors. Bioorg. Med. Chem. Lett. *14*, 2817–2822.

Bianco, P., Cao, X., Frenett, P.S., Mao, J.J., Robey, P.G., Simmons, P.J., and Wang, C.Y. (2013). The meaning, the sense and the significance: translating the science of mesenchymal stem cells into medicine. Nat. Med. *19*, 35–42.

Chang, J., Wang, Z., Tang, E., Fan, Z., McCauley, L., Franceschi, R., Guan, K., Krebsbach, P.H., and Wang, C.Y. (2009). Inhibition of osteoblastic bone formation by nuclear factor-kappaB. Nat. Med. *15*, 682–689.

Chang, J., Liu, F., Lee, M., Wu, B., Ting, K., Zara, J.N., Soo, C., Al Hezaimi, K., Zou, W., Chen, X., et al. (2013). NF-κB inhibits osteogenic differentiation of mesenchymal stem cells by promoting β-catenin degradation. Proc. Natl. Acad. Sci. USA *110*, 9469–9474.

Choo, A., and Lim, S.K. (2011). Derivation of mesenchymal stem cells from human embryonic stem cells. Methods Mol. Biol. *690*, 175–182.

Deng, P., Chen, Q.M., Hong, C., and Wang, C.Y. (2015). Histone methyltransferases and demethylases: regulators in balancing osteogenic and adipogenic differentiation of mesenchymal stem cells. Int. J. Oral Sci. *7*, 197–204.

Dreesen, O., and Brivanlou, A.H. (2007). Signaling pathways in cancer and embryonic stem cells. Stem Cell Rev. *3*, 7–17.

Dutta, D., Ray, S., Home, P., Larson, M., Wolfe, M.W., and Paul, S. (2011). Self-renewal versus lineage commitment of embryonic stem cells: protein kinase C signaling shifts the balance. Stem Cells *4*, 618–628.

Foldes, G., Liu, A., Badiger, R., Paul-Clark, M., Moreno, L., Lendvai, Z., Wright, J.S., Ali, N.N., Harding, S.E., and Mitchell, J.A. (2010). Innate immunity in human embryonic stem cells: comparison with adult human endothelial cells. PLoS One *5*, e10501.

Kang, H.B., Kim, Y.E., Kwon, H.J., Sok, D.E., and Lee, Y. (2007). Enhancement of NF-kappaB expression and activity upon differentiation of human embryonic stem cell line SNUhES3. Stem Cells Dev. *16*, 615–623.

Karp, J.M., Ferreira, L.S., Khademhosseini, A., Kwon, A.H., Yeh, J., and Langer, R.S. (2006). Cultivation of human embryonic stem cells without the embryoid body step enhances osteogenesis in vitro. Stem Cells *24*, 835–843.

Kern, S., Eichler, H., Stoeve, J., Kluter, H., and Bieback, K. (2006). Comparative analysis of mesenchymal stem cells from bone marrow, umbilical cord blood, or adipose tissue. Stem Cells *24*, 1294–1301.

Kode, J.A., Mukherjee, S., Joglekar, M.V., and Hardikar, A.A. (2009). Mesenchymal stem cells: immunobiology and role in immunomodulation and tissue regeneration. Cytotherapy *11*, 377–391.

Krum, S.A., Chang, J., Miranda-Carboni, G., and Wang, C.-Y. (2010). Novel functions for NFκB: inhibition of bone formation. Nat. Rev. Rheumatol. *6*, 607–611.

Li, O., Tormin, A., Sundberg, B., Hyllner, J., Le Blanc, K., and Sheding, S. (2013). Human embryonic stem cell-derived mesenchymal stroma cells (hES-MSCs) engraft in vivo and support hematopoiesis without suppressing immune function: implications for off-the shelf ES-MSC therapies. PLoS One *8*, e55319.

Luningschror, P., Stocker, B., Kaltschmidt, B., and Kaltschmidt, C. (2012). miR-290 cluster modulates pluripotency by repressing canonical NF-kappaB signaling. Stem Cells *30*, 655–664.

Park, B.K., Zhang, H., Zeng, Q., Dai, J., Keller, E.T., Giordano, T., Gu, K., Shah, V., Pei, L., Zarbo, R.J., et al. (2006). NF-κB in breast cancer cells promotes osteolytic bone metastasis by inducing osteoclastogenesis via GM-CSF. Nat. Med. *13*, 62–69.

Quarto, R., Mastrogiacomo, M., Cancedda, R., Kutepov, S.M., Mukhachev, V., Lavroukov, A., Kon, E., and Marcacci, M. (2001).

Repair of large bone defects with the use of autologous bone marrow stromal cells. N. Engl. J. Med. *344*, 385–386.

Ramadoss, S., Li, J., Ding, X., Al Hezaimi, K., and Wang, C.Y. (2011). Transducin beta-like protein 1 recruits nuclear factor kappaB to the target gene promoter for transcriptional activation. Mol. Cell. Biol. *31*, 924–934.

Stappenbeck, T.S., and Miyoshi, H. (2009). The role of stromal stem cells in tissue regeneration and wound repair. Science *324*, 1666–1669.

Thomson, J.A. (1998). Embryonic stem cell lines derived from human blastocysts. Science *282*, 1145–1147.

Torres, J., and Watt, F.M. (2008). Nanog maintains pluripotency of mouse embryonic stem cells by inhibiting NFkappaB and cooperating with Stat3. Nat. Cell Biol. *10*, 194–201.

Villa-Diaz, L., Brown, S., Liu, Y., Ross, A., Lahann, J., Parent, J., and Krebsbach, P. (2012). Derivation of mesenchymal stem cells from human induced pluripotent stem cells cultured on synthetic substrates. Stem Cells *30*, 1174–1181.

Wang, S., Qu, X., and Zhao, R.C. (2012). Clinical applications of mesenchymal stem cells. J Hematol. Oncol. *5*, 19.

Yang, F., Tang, E., Guan, K., and Wang, C.-Y. (2003). IKKβ plays an essential role in the phosphorylation of RelA/p65 on serine 536 induced by lipopolysaccharide. J. Immunol. *170*, 5630–5635.

Yang, C., Atkinson, S.P., Vilella, F., Lloret, M., Armstrong, L., Mann, D.A., and Lako, M. (2010). Opposing putative roles for canonical and noncanonical NFkappaB signaling on the survival, proliferation, and differentiation potential of human embryonic stem cells. Stem Cells *28*, 1970–1980.

Stem Cell Reports, Volume *6*

Supplemental Information

Inhibition of IKK/NF-κB Signaling Enhances Differentiation of Mesenchymal Stromal Cells from Human Embryonic Stem Cells

Peng Deng, Chenchen Zhou, Ruth Alvarez, Christine Hong, and Cun-Yu Wang

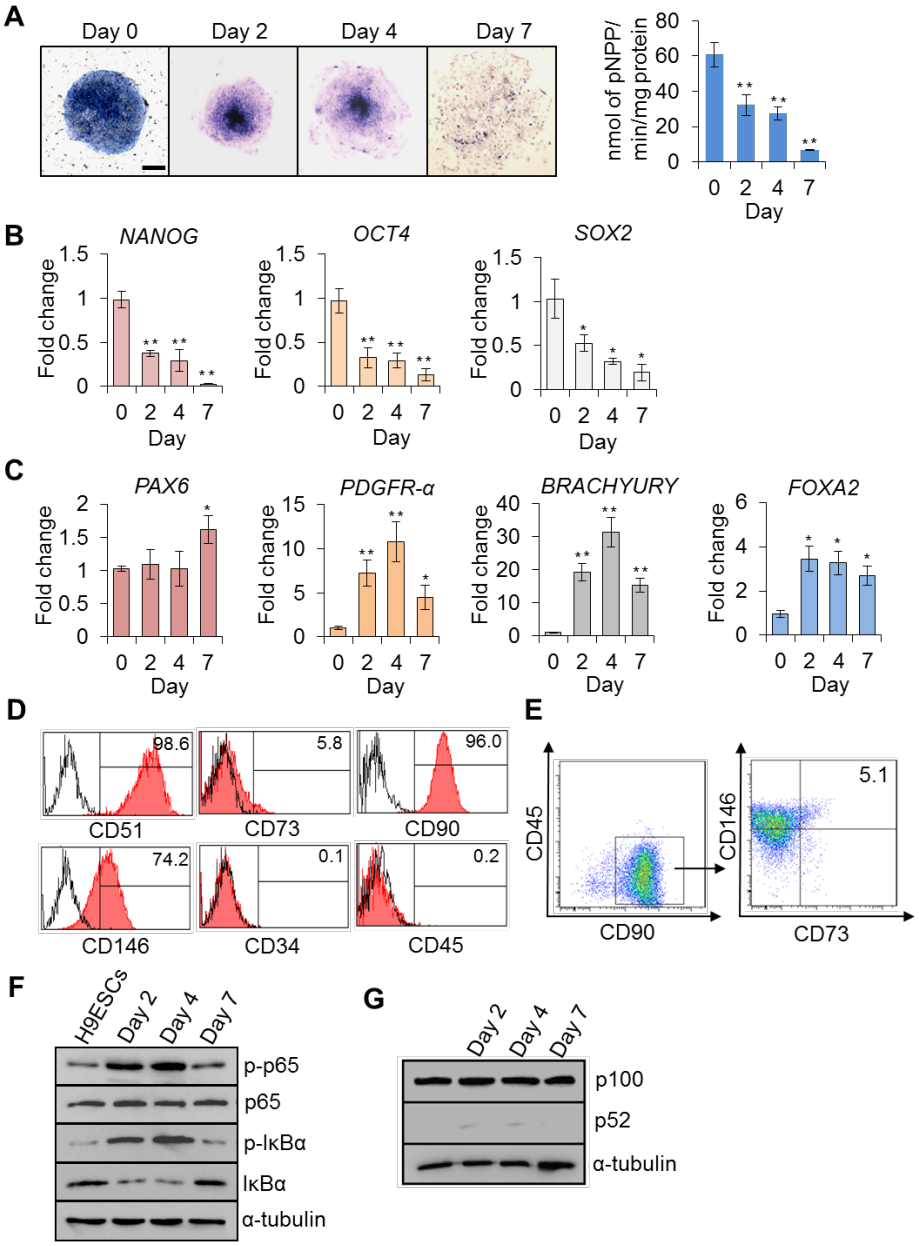

Figure S1. Spontaneous differentiation of H9 hESCs. Related to Figure 1. (A) ALP staining and quantitative ALP activity assay at 0, 2, 4, and 7 days. Bar indicates 200 μm. (B) qRT-PCR results of pluripotent markers (NANOG, OCT4, POU5F1) at 0, 2, 4, and 7 days. (C) qRT-PCR results of an ectodermal gene (PAX6), mesodermal genes (PDGFR-α and BRACHYURY), and an endodermal gene (FOXA2) at 0, 2, 4, and 7 days. (D) Flow cytometry analysis of cells expressing MSC surface markers. (E) Four-color flow cytometry analysis for CD45, CD90, CD73, CD146 expression was used to isolate $CD73^{+}CD90^{+}CD146^{+}CD45^{-}$ MSCs. (F) Western blot of both phosphorylated p65 and IκBα at 0, 2, 4, and 7 days of H9 hESC differentiation. (G) Western blot analysis of p100 and p52 at 0, 2, 4, and 7 days of H1 hESC differentiation. Three independent experiments were performed. * $p < 0.05$, ** $p < 0.001$.

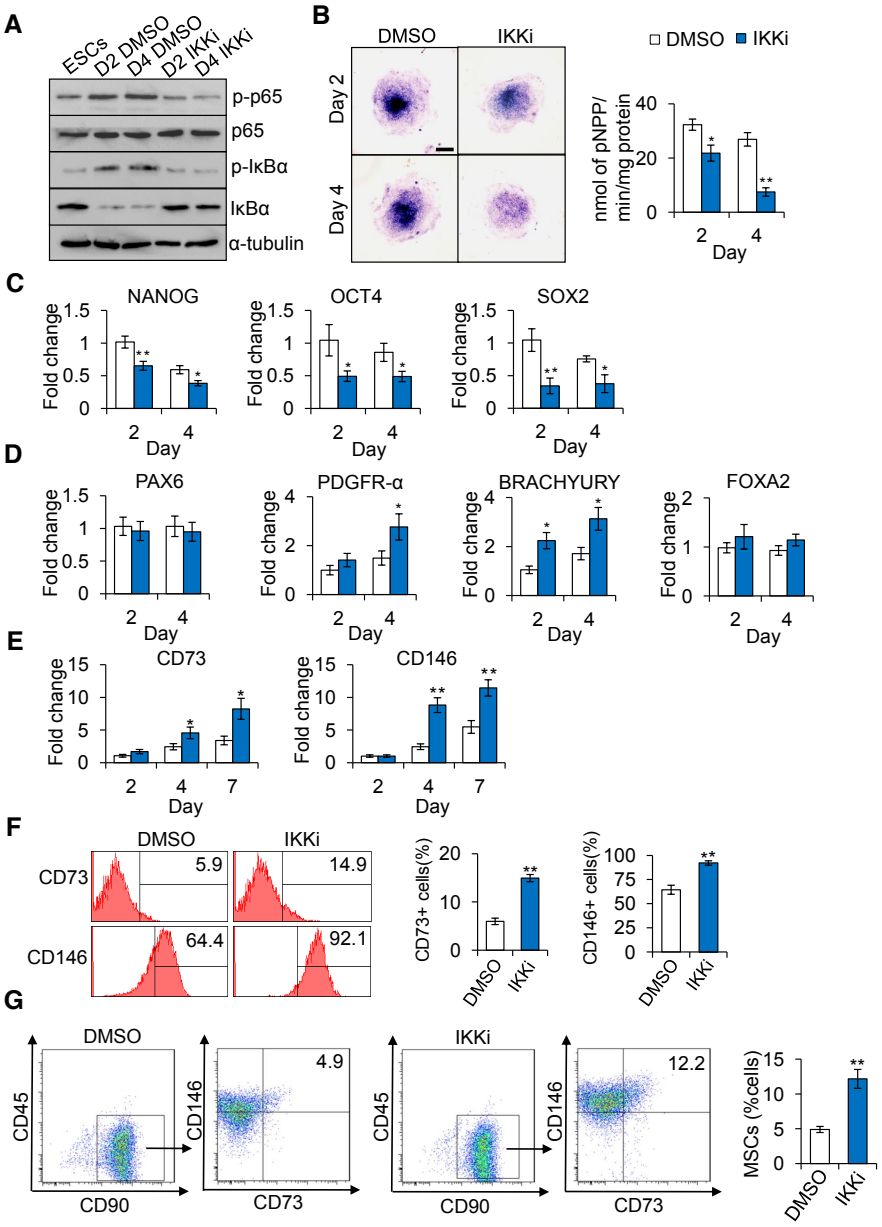

Figure S2. Effect of IKKi treatment on mesenchymal lineage specification of H9 hESCs. Related to Figure 2. (A) Western blot of p65, phosphorylated p65, IκBα and phosphorylated IκBα at 0, 2, and 4 days of H9 hESC differentiation. (B) ALP staining and quantitative ALP activity assay at 2 and 4 days. Bar indicates 200 μm. (C) qRT-PCR results of *NANOG, OCT4, POU5F1* at 2 and 4 days. (D) qRT-PCR results of *PAX6*, *PDGFR-α, BRACHYURY*, and *FOXA2* at 2 and 4 days. (E) qRT-PCR results of *CD73* and *CD146* at 2, 4, and 7 days. (F) Flow cytometry analysis of cells with or without IKKi treatment examining MSC marker expression. (G) Four-color flow cytometry analysis for CD45, CD90, CD73, CD146 expression to isolate $CD73^{+}CD90^{+}CD146^{+}CD45^{-}$ MSCs following 7 days of H9 hESC differentiation with or without IKKi. Proportions of $CD73^{+}CD90^{+}CD146^{+}CD45^{-}$ MSCs generated. Three independent experiments were performed. * $p < 0.05$, ** $p<0.001$.

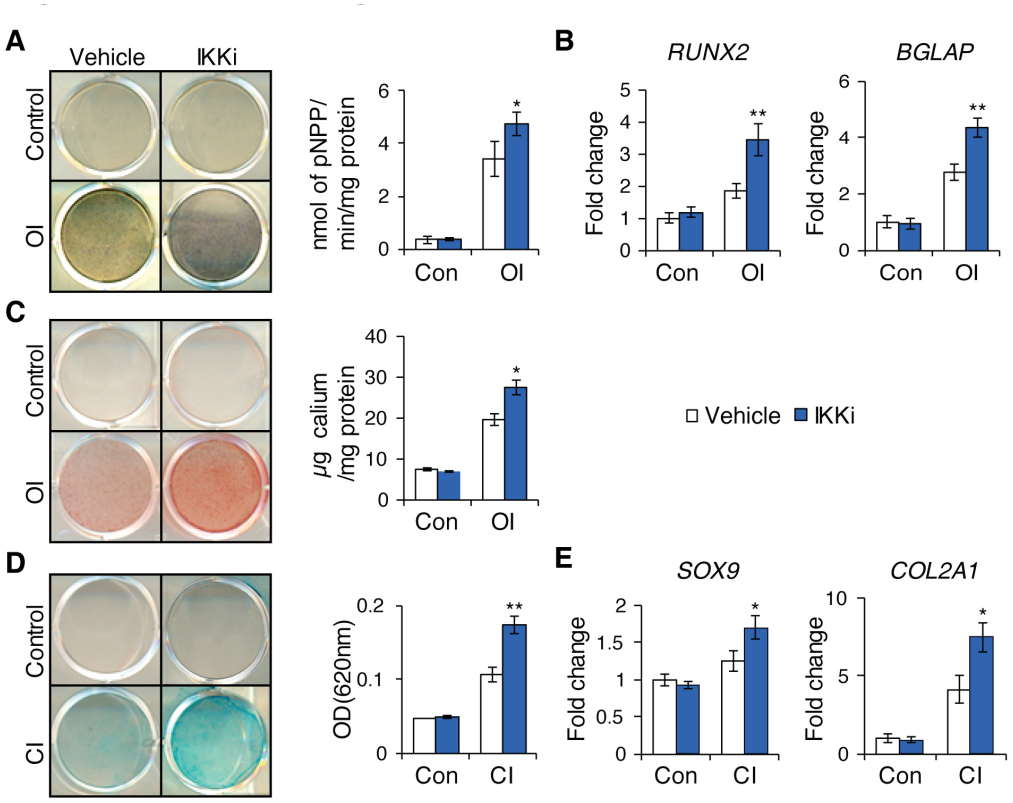

Figure S3. Osteogenic and Chondrogenic differentiation potential of differentiated hESCs with or without IKKi treatment. Related to Figure 2. After 7 days of differentiation, hESCs with or without IKKi treatment were digested by trypsin to generate a single-cell suspension. To test the differentiation potential of these cells, they then were seeded into plates, and cultured in induction medium as indicated. (A) ALP staining and quantitative ALP activity assay after 14 days of osteogenic induction (OI). (B) qRT-PCR results of osteogenic markers (*RUNX2* and *BGLAP*) after 7 days of OI. (C) ARS staining and quantification after 14 days of OI. (D) Alcian blue staining and quantification of derived cells with DMSO or IKKi treatment after 21 days of chondrogenic induction (CI). (E) qRT-PCR results of chondrogenic markers (*SOX9* and *COL2A1*) after 14 days of CI. For all *in-vitro* experiments, three independent experiments were performed. * $p < 0.05$, ** $p < 0.001$.

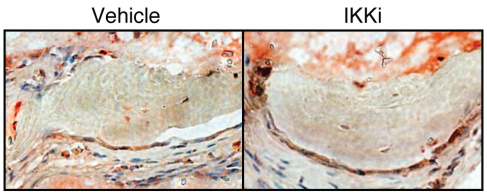

Figure S4. Osteocalcin staining of ectopic bone *in vivo* by sorted MSCs derived from IKKi-treated H1 hESCs. Related to Figure 4.

Table S1. Primers for RT-PCR

Name	Forward	Reverse
GAPDH	GGAGCGAGATCCCTCCAAAAT	GGCTGTTGTCATACTTCTCATGG
NANOG	CTGGCTGAATCCTTCCTCTC	CATGAGATTGACTGGATGGG
SOX2	GCGAACCATCTCTGTGGTCT	GGAAAGTTGGGATCGAACAA
OCT4	GAAGGATGTGGTCCGAGTGT	GTGAAGTGAGGGCTCCCATA
PAX6	TGGGCAGGTATTACGAGACTG	ACTCCCGCTTATACTGGGCTA
PDGFR-α	TATGTGCCAGACCCAGATGT	GGAGTCTCGGGATCAGTTGT
BRACHYURY	TATGAGCCTCGAATCCACATAGT	CCTCGTTCTGATAAGCAGTCAC
FOXA2	GGAGCAGCTACTATGCAGAGC	CGTGTTCATGCCGTTCATCC
CD73	TTACACAGGCAATCCACCTTC	TTACACAGGCAATCCACCTTC
CD146	CTGCTGAGTGAACCACAGGA	CACCTGGCCTGTCTCTTCTC
cIAP2	CCTAGCTGCAGATTCGTTCA	GAGCCACGGAAATATCCACT
IL-6	GGCACCTCAGATTGTTGTTG	TAAGTTCTGTGCCCAGTGGA
IL-8	ATGACTTCCAAGCTGGCCGTG	TCTCAGCCCTCTTCAAAAACTTCTC

Supplemental Experimental Procedures

Induction of Osteogenic, Chondrogenic, and Adipogenic Differentiation

To induce osteogenic differentiation, cells were grown in osteogenic induction (OI) medium containing 1nM dexamethasone, 100μM ascorbic acid, and 5mM beta-Glycerophosphate. To induce chondrogenic differentiation, cells were cultured in chondrogenic induction (CI) medium containing 100mM sodium pyruvate, 40μg/mL proline, 100nM dexamethasone, 200μM ascorbic acid, and 10ng/mL TGF-β3. To induce adipogenic differentiation, the cells were cultured in adipogenic induction (AI) medium containing 1μM dexamethasone, 10μg/mL insulin, 0.5 mM 3-isobutyl-1-methylxanthine, and 0.2mM indomethacin. Media was changed every 2 days.

ALP, Alizarin Red Staining, Alcian Blue Staining and Oil-Red O Staining

1x 10^5 cells were seeded into each well in 12-well plates for further differentiation and staining. ALP activity assay and ARS were performed as described previously after 7 days and 14 days of osteogenic differentiation respectively (Chang et al., 2009). After 3 weeks of chondrogenic differentiation, Alcian blue staining was performed. Cells were fixed with 10% neutral buffered formalin for 15 min at room temperature, and then incubated in Alcian blue staining solution (1% Alcian blue in 3% Acetic acid) for 30 min. For quantification, stained Alcian blue was eluted with 6 M guanidine HCl for 6 hrs at room temperature. The optical absorbance was measured at 650 nm using a microplate reader. After 21 days of adipogenic induction, Oil-Red-O staining was performed using an OIL-RED-O STAIN KIT according to the manufacturer's instructions (Diagnostic BioSystems, Pleasanton, CA, USA). For quantification, stained Oil-Red-O was eluted with 100% isopropanol and the optical absorbance was measured at 450nM using a microplate reader.

Quantitative Reverse Transcriptase-Polymerase Chain Reaction (qRT-PCR)

Total RNA was isolated from ES-MSCs using Trizol reagents (Invitrogen). Two-μg aliquots of RNA were synthesized using random hexamers and reverse transcriptase according to the manufacturer's protocol (Invitrogen). qRT-PCR was performed using the QuantiTect SYBR Green PCR kit (Qiagen) and the Icycler iQ Multi-color Real-time PCR Detection System (BioRad) and normalized to GAPDH. Data shown are representative of three independent experiments. Primer sequences are listed in Table

S1.

Western Blot Analysis

Protein was isolated from cells using CelLytic MT solution (Sigma), supplemented with protease inhibitor cocktail (PIC, Promega, Southampton, USA). 40 µg aliquots of protein were separated by a 7.5% SDS-polyacrylamide (PAGE) gel. The following primary antibodies and reagents were used: rabbit anti-human phosphorylated p65-S536 (#3033S, Cell Signaling, Danvers, MA, USA), rabbit anti-human p65 (SC-109, Santa Cruz Biotech, Dallas, Texas, USA), rabbit anti-human phosphorylated IκBα (2859, Cell Signaling), rabbit anti-human phosphorylated IκBα-S32 (2859, Santa Cruz Biotech), rabbit anti-human p100 and p52 (4882, Cell Signaling), mouse anti-human α-tubulin (SC-8035, Santa Cruz Biotech, Dallas, Texas, USA). Detection was performed with using Luminal/Enhancer Solution and Super Signal West Stable Peroxide Solution (Thermo). Blots were then exposed to HyBlot CL autoradiography films (Denville Scientific, South Plainfield, NJ, USA).

Immunohistochemistry (IHC)

Paraffin-embedded sections were performed by the UCLA Translational Pathological Core Laboratory. Samples were deparaffinized with xylene and rehydrated with distilled water through an ethanol series. Tissue antigen retrieval was carried out and immunohistochemistry were performed by using EnVision system (DAKO, Carpinteria, CA, USA) according to the manufacturer's instructions. Rabbit anti-human osteocalcin antibody (1:100; SC-30044) was purchased from Santa Cruz Biotechnology. The section counterstained with hematoxylin QS (Vector Laboratories, Burlingame, CA, USA), and at least three pictures of each sample were taken randomly (Olympus).

Flow Cytometry and Fluorescence-Activated Cell Sorting (FACS)

Cells were digested with trypsin (Invitrogen) for 2 min at 37°C, neutralized and passed through a 40 µm cell strainer. Then, cells were washed twice with FACS buffer (PBS, 10 mM EDTA, and 2% FBS) and resuspended at a maximum concentration of 2 x 10^5 cells per 100 µ l. Cells were stained with indicated antibodies for 30 min on ice in dark, washed, and resuspended in PBS. Samples were analyzed on a BD LSR II analyzer or sorted on a BD FACS Aria III. Cell gating was based on comparison with isotype negative controls and single stained controls. Cells were sorted into serum-free DMEM

media for gene expression analysis or into complete media for cell culture. Antibodies used include CD34 (PE; 316407), CD45 (PerCP-Cy5.5; 103234), CD51 (PE; 327910), CD73 (APC; 344006), CD90 (FITC; 328108), CD146 (PE; 342004) (Biolegend, London, UK).

Transplantation in Immunocompromised Mice

All procedures were performed in accordance with the approved protocol by the University of California, Los Angeles (UCLA), and were oversight by UCLA Animal Research Committee (ARC). Briefly, sorted MSCs (1×10^6) were mixed with 40 mg of hydroxyapatite/tricalcium phosphate (HA/TCP) scaffolds and then transplanted subcutaneously in 8-week-old nude mice (n=6). Sorted ES-MSCs derived from vehicle-treated hESCs were transplanted into the left dorsal subcutaneous sites and sorted MSCs derived from IKKi-treated H1 hESCs were transplanted into the left dorsal subcutaneous sites. Eight weeks after transplantation, the transplants were collected. H&E staining was performed and at least three pictures of each sample were taken randomly (Olympus). For quantification of mineralized tissue, SPOT 4.0 software (Diagnostic Instruments) was used to measure the area of mineralized tissue versus total area.